



ELSEVIER

Available online at [www.sciencedirect.com](http://www.sciencedirect.com)

SCIENCE @ DIRECT®

Cold Regions Science and Technology 43 (2005) 93–103

cold regions  
science  
and technology

[www.elsevier.com/locate/coldregions](http://www.elsevier.com/locate/coldregions)

# Improvement of a numerical snow drift model and field validation

Yves Durand <sup>\*</sup>, Gilbert Guyomarc'h, Laurent Mérindol, Javier G. Corripio <sup>1</sup>

*Météo-France, Centre d'Études de la Neige, 1441 rue de la Piscine, 38406 Saint Martin d'Hères, France*

Received 21 August 2004; accepted 22 May 2005

## Abstract

For about ten years, Météo-France has developed and operated a real time operational suite aimed at snowpack simulation and avalanche risk forecasting: the numerical model chain Safran-Crocus-Meptra (SCM). It presently includes only a crude formulation of snowdrift effects at large spatial scales (massif). This paper presents the improvements to a snow drift module suited to the SCM chain. The new version, called SYTRON3 which aims at an improved simulation of snow drift effects at smaller spatial scales. It is coupled with the SCM environment, which provides hourly meteorological conditions and snow forcing. The main modifications concern the new parameterisation schemes, which are more realistic and more physically based. The increased number of vertical layers allows now to represent explicitly the three modes of movement during snow drift: creep, saltation and diffusion. The validation of this new version as well as comparisons with the previous version are performed at the Col du Lac Blanc test site (2700 m a.s.l., French Alps) by the use of digital photographs and field observations. © 2005 Elsevier B.V. All rights reserved.

*Keywords:* Snow drift; Model validation; Avalanche risk

## 1. Introduction

The importance of snow drift effects on snow-covered mountain surfaces has been identified long ago. Its consequences affect both mountain economic activities and the safety of many users and professionals due to its great influence on snow redistribution and avalanche activity. This is why these effects

have to be taken into account for the operational real-time snowpack modelling at different spatial scales. In order to achieve this goal and to improve the current operational snowpack and avalanche risk forecasting numerical model chain Safran-Crocus-Meptra (SCM) (Durand et al. (1999), a numerical parameterisation of snow drift effects at a finer spatial scale ( $\sim 1 \text{ km}^2$ ) than presently (massif scale, about  $400 \text{ km}^2$ ) was incorporated. The previously developed model SYTRON2 was described in Durand et al. (2001, 2004). This preliminary version was based on very simplified flux formulations and soon the need for a more sophisticated model emerged. The new version SYTRON3, keeps the same running constraints: i.e.

<sup>\*</sup> Corresponding author.

*E-mail address:* [Yves.Durand@meteo.fr](mailto:Yves.Durand@meteo.fr) (Y. Durand).

<sup>1</sup> Present address: Swiss Federal Institute of Technology, IHW-ETH, Wolfgang Pauli Strasse 15, Honggerberg HIL g 28.1, CH-8093 Zurich, Switzerland.

initialisation and input fields provided by the real time SCM chain and short computer run time, but with improved schemes. Its validation is based on digital photographs of our test site (Col du Lac Blanc, 2700 m a.s.l., French Alps) taken from a nearby point overlooking the study area. A special treatment of the photographs (Corripio et al., 2004) allows to derive several surface parameters such as observed relative albedo or features indicating snow drift effects.

## 2. State of the art on numerical modeling of snow drift

Snow transport by wind remains an open research field especially for real-time numerical simulations. The complexity of the phenomena involved, their large range of spatial scales, the mutual interaction between different processes, and the equilibrium state between the snow and the air flux make the snow drift problem very difficult to treat and solve accurately. Numerical modelling of snow drift has been an active research field for many years now. In the following we do not aim at an exhaustive review, but will only mention the studies that are directly relevant for our model development.

Pomeroy and Gray (1990) designed a very useful semi-empirical saltation model well suited for flat areas. Subsequently, it was also used by Liston and Sturm (1998) to perform long term simulations without any explicit treatment of the snow crystal characteristics. Naaim et al. (1998) developed a model based on continuum theory of erosion and deposition fluxes in order to simulate wind tunnel experiments. Gauer (2001) and Lehning et al. (2002) designed successful attempts combining wind field and snow modelling and sophisticated phenomena descriptions at the expense of important computer costs. We designed a one-layer snow drift model, called SYTRON2, in order to simulate on a limited mountainous area the main fine scale structures (about 1 km) due to snow drift during a limited period of time (a few hours). The model is coupled every hour with the SCM output through appropriate downscaling procedures and aims at representing the occurrence of blowing snow and the total snow mass transported and sublimated. However, the main weakness of the model is the internal parameterisation which is too empirical (Durand et al., 2001, 2004).

The work presented below is inspired by the above-mentioned papers and can be seen as a synthesis of these contributions. They were compared to our own field experience in order to build a functional scheme allowing the real-time numerical simulation to be coupled with the operational forecasting model chain (SCM).

## 3. Numerical formulation “SYTRON3”

### 3.1. Presentation

The aim of the new formulation is to make the previous version (SYTRON2) more physically based by including more realistic relations based on more rigorous assumptions especially for the erosion processes. The SYTRON2 model was too much empirically based. It reproduced the field observations at our test site, but could not be generalised to other locations due to the lack of fundamental elements involved in the different processes. For the new version, we mainly build on the work of Naaim et al. (1998) and Pomeroy and Gray (1990) and adapted it for our purpose. The objectives were to achieve a fast computer run and to use the daily operational results of the SCM chain (Durand et al., 1999) as input data. A horizontal grid size of about 45 m is used. However, the large size of the grid cells makes the comparison with observed snow drift events difficult. This is mainly due to the great range of spatial scales of the phenomenon. The smallest scale which is induced by micro topography, is not taken into account, and neither is its evolution nor its interaction with larger scales.

### 3.2. Determination of vertical layers

Contrary to SYTRON2, with only one averaged vertical layer, the new model uses three numerical vertical layers in order to better represent creep, saltation and turbulent diffusion. The saltation height  $h_2$  (m) is estimated following Greely and Iversen (1985), a formulation which was also used by Liston and Sturm (1998):

$$h_2 = 1.6 \frac{u_*^2}{2g} \quad (1)$$

where  $u_*$  ( $\text{m s}^{-1}$ ) is the friction velocity which characterizes the shear stress exerted on the snow by the

wind and  $g$  ( $\text{m s}^{-2}$ ) is the gravitational acceleration. The other heights are 1 cm ( $h_1$  for creep) and 10 m ( $h_3$  for turbulent diffusion), which have been fixed according to values taken from the literature and to our own field observations.

### 3.3. Initial wind field and occurrence of drift

The wind model SAMVER as well as its statistical correction (Durand et al., 2004) have not yet been upgraded. It simulates the temporal evolution of the potential vorticity and of the divergence of a 2D wind field on an isentropic surface near the surface. It is used as an operator to adjust the wind field to the orography and provides only one vertical level of wind field estimation with two components that result in a speed  $u_r$  ( $\text{ms}^{-1}$ ) at a height ( $z_r$ ) of about 7.5 m corresponding to the initial conditions provided by SAFRAN (Durand et al., 2001, 2004). As in the previous version, the wind estimation will be kept constant for periods of one hour and will be used for the local computation of the particle velocity within the three vertical layers.

Under the classical assumption of neutral conditions in a boundary layer with constant fluxes, we get an initial relation between  $u_*$  and  $z_0$

$$u_* = u_r \frac{\kappa}{\ln(z_r/z_0)} \quad (2)$$

where  $\kappa$  is the von Karman constant and  $z_0$  (m) is the roughness length.

The occurrence of snow transport is determined by the PROTEON method (Guyomarc'h and Mérindol, 1998), which uses both the velocity  $u_r$  and the snow crystal characteristics at the snow surface to determine a snow mobility index (SI). A positive value indicates drift occurrence. As previously described by Gallée et al. (2000), the index gets a zero value for the threshold wind velocity  $u_{rt}$  at which snow drift starts. Assuming the same boundary layer conditions and the same elevation  $z_r$  for  $u_{rt}$ , we get the threshold friction velocity  $u_{*t}$  from Eq. (2) as:

$$u_{*t} = u_{rt} \frac{u_*}{u_r} \quad (3)$$

### 3.4. Estimation of advection wind field for the different layers

Particle velocity is finally computed depending on the local occurrence of transport. If occurrence is suggested by the PROTEON model ( $SI > 0$ ), we assume, following Owen (1964) and Liston and Sturm (1998), a coupling between  $u_*$  and  $z_0$ :

$$z_0 = 0.12 \frac{u_*^2}{2g} \quad (4)$$

The Eqs. (2) and (4) allow the determination (by an iterative descending method) of  $u_*$  and  $z_0$ . The inverse form of Eq. (2) is used to obtain, by vertical integration into the three vertical layers  $[0, h_1]$ ,  $[h_1, h_2]$ ,  $[h_2, h_3]$ , a first guess of the particle velocities:  $u_1$  (creep),  $u_2$  (saltation),  $u_3$  (diffusion). The corresponding wind directions are not changed from the initial SAMVER values. If no drift occurrence is suggested by PROTEON ( $SI \leq 0$ ), a constant roughness length  $z_0$  of 0.005 m is assumed and Eq. (4) is not used.

### 3.5. Erosion fluxes and advection velocity

It is well known (e.g. Kind, 1976; Naaim et al., 1998) that snow transport occurs mainly during a steady state resulting from the mutual interactions between the wind and the snow surface. We assume that the shear stress remains at its threshold value as long as snow erosion is possible. This steady state is characterized by a maximum amount  $m_m$  ( $\text{kg m}^{-2}$ ) of snow by surface area and which moves inside the layer and is determined by the relationship deduced from Pomeroy and Gray (1990):

$$m_m = \gamma \rho \frac{u_*^2 - u_{*t}^2}{g u_*} \quad (5)$$

where  $\rho$  ( $\text{kg m}^{-3}$ ) is the density of air and  $\gamma$  is a constant which was assumed to be  $\gamma = 0.243 \text{ m s}^{-1}$  according to Pomeroy and Gray (1990). The expression  $\gamma/u_*$  characterizes the efficiency of the saltation process. The quantity  $m_m$  is only computed at places where erosion is possible. At first order, the erosion flux is proportional to an adapted excess shear stress and, as described in Naaim et al.

(1998), can be formulated in terms of a mass variation  $m_e$  ( $\text{kg m}^{-2}$ ):

$$\delta m_e / \delta t \approx (u_{*r}^2 - u_{*t}^2) \quad (6)$$

with  $u_{*r}$  ( $\text{m s}^{-1}$ ) being an adapted friction velocity, defined subsequently. The steady state is assumed by adjusting the vertical erosion fluxes (the deposition fluxes are fixed) in order to maintain the snow mass in movement at its maximum value  $m_m$  whenever possible. This is achieved by using an adapted form  $u_{*r}$  of the friction velocity which takes implicitly into account the equilibrium between snow and air and hence is representative of the new fluid in movement composed of snow and air. Eq. (6) is thus applied as:

$$\delta m_e / \delta t = A\rho(u_{*r}^2 - u_{*t}^2) \quad (7)$$

$$u_{*r} = u_* + (u_{*t} - u_*) \left( \frac{m_2}{m_m} \right)^2 \quad (8)$$

with  $m_2$  ( $\text{kg m}^{-2}$ ) being the actual snow mass in movement into the cell inside the saltation layer and  $A$  a constant depending on the snow surface structure. The main practical difficulty of applying Eq. (7) comes from the fact that the snow profile is divided into different layers of different characteristics and so the total extracted mass can be extracted from several layers and must be aggregated with the snow quantity already moving.

The same method is also applied to modify the advection velocity within the lower layers. As indicated by Pomeroy and Gray (1990), and also used by Liston and Sturm (1998), the horizontal particle velocity  $u_p$  within the saltation layer can be considered as constant and approximated by:

$$u_p = 2.8u_{*t}. \quad (9)$$

Assuming such a value during the steady state drift event and hence taking into account that the fluid velocity slows down due to the presence of snow particles, the wind velocity inside the creep and saltation layers is corrected as:

$$u_{2\text{corr}} = u_2 \left( 1 - \left( \frac{m_2}{m_m} \right)^2 \right) + u_p \left( \frac{m_2}{m_m} \right)^2$$

$$u_{1\text{corr}} = u_1 \frac{u_{2\text{corr}}}{u_2}. \quad (10)$$

At each time step, the total eroded snow mass  $\delta m_e$  is split into the three vertical layers and into a sublimated part. No precise studies or clear experiment allow to determine the amount of snow in the creep layer. Additionally, we assume the occurrence of creep only when saltation occurs as well. This assumption is obviously wrong and even contrary to our own observations. For simplification, the snow mass remaining in the creep layer  $\delta m_1$  ( $\text{kg m}^{-2}$ ) is assumed to be:

$$\delta m_1 = B \delta m_e \quad (11)$$

with the constant  $B$  arbitrarily set to 0.1. This assumption implies that the snow quantities for the saltation layer  $\delta m_2$  ( $\text{kg m}^{-2}$ ), diffusion layer  $\delta m_3$  ( $\text{kg m}^{-2}$ ) and sublimation  $\delta m_s$  ( $\text{kg m}^{-2}$ ) are linked as:

$$\delta m_2 + \delta m_3 + \delta m_s = (1 - B)\delta m_e. \quad (12)$$

Greatly simplifying the scheme proposed by Kind (1992) which was also used in refined form by Liston and Sturm (1998), we assumed that the mass concentrations inside the layers were linked as:

$$\delta m_3 = C \delta m_2 \frac{h_3 - h_2}{h_2 - h_1}$$

$$\delta m_s = w D \delta m_3$$

$$w = u_3 \sin(\alpha) \quad (13)$$

with  $w$  ( $\text{m s}^{-1}$ ) being a crude estimation of the vertical velocity obtained from the slope angle  $\alpha$  along the horizontal flux direction. The constant  $C$  is obtained by vertically averaging (from  $h_2$  to  $h_3$ ) the expression for the concentration of blowing snow within the turbulent suspension layer as used by Liston and Sturm (1998, Eq. (11)). The same formulation is used and the integration starts with the saltation concentration at the lowest level. The variable  $D$  ( $\text{s m}^{-1}$ ) was also introduced by Liston and Sturm (1998), themselves inspired by other authors; it represents an averaged coefficient of sublimation loss rate (Liston and Sturm, 1998; Eq.s A-2 to A-5). The values of  $C$ ,  $D$  and  $w$  are computed at each vertical layer where erosion occurs and the Eqs. (12) and (13) allow to determine the mass input into the three vertical layers as well as the sublimation losses.

### 3.6. Deposition fluxes

Contrary to Naaim et al. (1998), we do not assume a deposition equal to zero when  $u_* \geq u_{*t}$ . The scheme ensures at the same time step both erosion and deposition in order to simulate roughly the snow particle trajectories and the shape modifications resulting from the drift process. The previous scheme in SYTRON2 is kept but modulated according to the deviation between  $u_*^2$  and  $u_{*t}^2$ . The initial deposition rate increases when  $u_* < u_{*t}$  and decreases otherwise.

### 3.7. Snow crystal shape modification

SYTRON3 uses the same parameterisation as SYTRON2 for the drift induced grain shape modification. Snow drift leads to slightly rounded crystals of smaller size and with reduced dendricity forming layers of increased snow density. The modifications are performed at each time step and are a generalization of the scheme used in the operational SCM forecasting model chain (Durand et al., 1999). In this chain, snow transport by wind is not explicitly modelled, and the hourly rate of crystal modification only depends on wind velocity because the initial snow shape is always the one of fresh precipitation particles. Our adaptation allows the use of any initial crystal shape, representative of the eroded snow, and the slight modification of these crystals with transformation rates comparable to those used in the SCM forecasting model chain. The transformation processes are all pointing at a final stage defined by zero dendricity, full sphericity and a minimum size of 0.4 mm. The freshly fallen snow undergoes the same modifications as in the SCM forecasting model chain. Previously metamorphosed and deposited snow is also modified such that it tends to the state of small rounded grain.

## 4. Field validation

### 4.1. Study site

In order to assess the performance of SYTRON3, measurements and observations were carried out at the well-instrumented site of Col du Lac Blanc (French Alps, 2700 m a.s.l., Fig. 1). This mountain



Fig. 1. Original photographic image taken from Pic Blanc (3323 m a.s.l.). North is right.

pass is a relatively flat area between the Pic Blanc (3323 m a.s.l.) and the Dôme des Petites Rousses (2810 m a.s.l.). It presents a natural corridor between these two peaks oriented roughly north-south. This corridor shape produces a tunnelling effect on the wind, which is often rather strong during the winter months with evident snow transport. The experimental area is equipped with two automatic weather stations recording every 15 min the measurements of specific parameters related to snow drift events and a horizontal profile of snow stakes where snow accumulation or erosion can be manually observed with a precision of 10 cm.

### 4.2. Methodology

Each version of SYTRON is evaluated for the experimental site to assess the performance and to validate the applicability. In addition to nivo-meteorological stations, several specific sensors and a range of snow stakes, and a novel remote sensing technique based on terrestrial photography is applied. The choice of this technique is a compromise between feasibility of implementation and efficiency.

Measuring variations of snow depth over large areas (several km<sup>2</sup>) is not a trivial task. Most remote sensing techniques do not have the requested precision which is of the order of a few cm when averaged over the output area of a model grid cell of 45 m × 45 m. Potentially precise methods include radar, which may have difficulties with dry snow, 3D laser altimetry, which is very expensive, and photogrammetry, which already has been applied at the experimental site and has shown very poor results (Castelle, 1995).

We choose as method an indirect measurement of snow surface changes. Oblique digital photographs of the area are taken periodically and after snow drift events from an elevated point. These photographs are then geo-referenced to a digital elevation model. Further radiometric corrections depending on topography and atmospheric conditions are applied to the geo-referenced pixels to derive relative albedo. Spectral filtering (in order to obtain near IR photography) applied to the digital camera permits detecting small variations in the associated snow grain characteristics (Wiscombe and Warren, 1980). The effects of snow transport by wind, erosion, accumulation and snow grain characteristics described by the model can be compared to changes in albedo, texture and features variations as recorded by the photographs.

The result of the processing described above is a map of reflectance values (normalized for insolation and topography). By comparing this map to a pixel of reference we can deduce the relative albedo of the whole visible area (Corripio, 2004; Corripio et al., 2004). These albedo values are then compared to those derived from SYTRON modelling outputs.

This new tool seems to be an appropriate technique for spatial validation of snow drift modelling. It is useful in identifying both strengths and weaknesses of the model, and the contribution of the new improved version.

#### 4.3. Results

From December 2003 to May 2004, 17 sets of photographs were taken. Eight of them were taken immediately after a snow drift period without precipitation, as soon as the weather conditions were appropriate (visibility and clear sky). These photographs were taken from three different points overlooking the Col du Lac Blanc site. Information on these periods is complemented by different automatic observation sources as described above. Manual observations during these events were done as well, and SYTRON2 and SYTRON3 model runs were performed.

A comparison between photographs and modelling results is presented for 24 February 2004. Fig. 2a shows the relative albedo derived from a digital photography (Fig. 1) taken from the Pic Blanc (3320 m a.s.l.), looking west to the Col du Lac Blanc. Fig. 2b

and c show the albedo derived respectively from SYTRON2 and SYTRON3 for the corresponding area. The triangular shape of the figures is due to the planar projection of the conical field of view of the camera. Black areas inside the coloured images are non-visible areas, hidden behind cliffs or steeper slopes or masked out due to very low illumination or viewing angles. The colour table is stretched and contrasted to highlight the differences. The albedo values are relative: red indicating high albedo and blue low albedo. The meteorological conditions at the time of image acquisition are characterized by moderate winds (velocity around  $10 \text{ m s}^{-1}$ , south direction), and air temperature around  $-5 \text{ }^\circ\text{C}$ . Snow accumulation since the previous day was  $10^{-15} \text{ cm}$  and a moderate snow transport by wind was observed in the previous hours.

Considering the horizontal difference in resolution between the photography (1 m) and the simulation (45 m), we focus on the main general patterns of albedo. For instance, some details visible on the photographic interpretation of albedo such as the lower values of albedo due to rocks in the bottom left-hand corner are obviously not visible in the image derived from the simulation because the area covered by rocks is smaller than the model resolution. The projection of the cableway cables is also visible. Nevertheless, in this case, the two models exhibit similar results even if SYTRON3 shows overall a better agreement with the photographic image than SYTRON2. This is probably due to a better representation of the snow layers near the snow surface. At this period of season, the snow surface conditions are often more favourable for this type of study thanks to a greater variety of snow particle types that produce an enhanced contrast in snow surface reflectance. The precipitation particles fell on a snow surface consisting of large rounded grains which had undergone melt-freeze metamorphism. In this case, the red areas mostly represent accumulation zones and the blue areas represent erosion zones due to the reappearance of layers of melt-freeze grains after the snow drift event.

Also for 24 February 2004, Fig. 3a and b show the modelled snow depth differences during the snow drift event for SYTRON2 (a) and SYTRON3 (b) with a bold triangle indicating the photographic

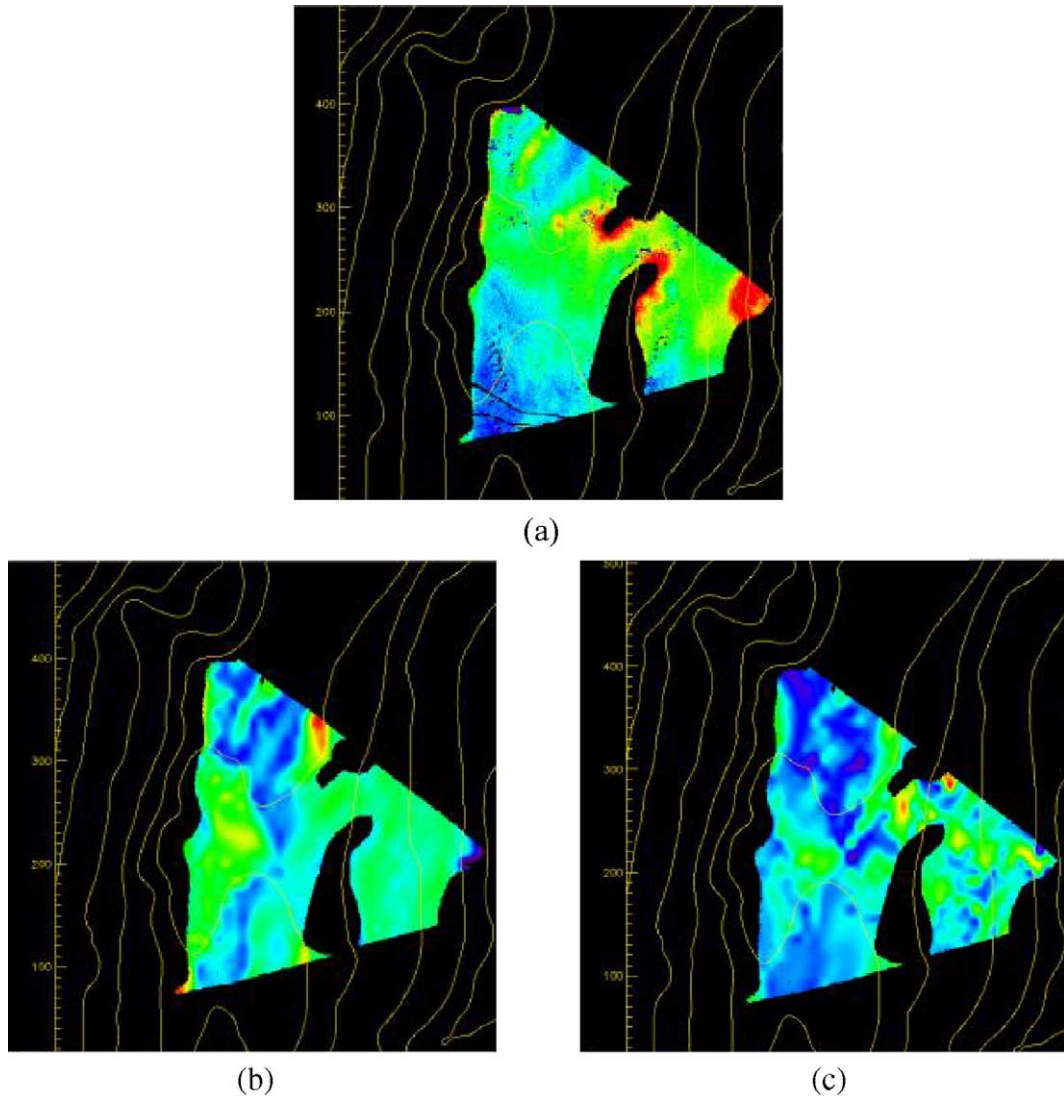


Fig. 2. Comparisons between different relative albedo maps : red values indicate high albedo and blue values indicate low albedo. (a) shows the relative albedo derived from a digital photography (Fig. 1) taken from the “Pic Blanc” (3323 m a.s.l.) looking west to the “Col du Lac Blanc”. (b) and (c) show the albedo derived from SYTRON2 and SYTRON3, respectively, for the same corresponding area and date. The area shown represents about  $2.5 \text{ km} \times 2.5 \text{ km}$ , the contour lines are 100 m apart. North is towards the top.

view. Roughly similar features can be observed in the two figures. The similarity follows from results presented in Fig. 2 and is due to the use of PROTEON in both our two models, even if the erosion processes are different. However, SYTRON2 shows larger patterns and overall less small-scale details with locally larger amounts of both accumulation and erosion. These characteristics of SYTRON2

come from the lack of an imposed steady-state saltation that limits the maximum amount of snow that can be transported (see Eq. (5)).

We tried to check the modelled snow depth differences with the recorded field data. SYTRON3 exhibits a significant difference to SYTRON2 at the location of one of the snow depth sensors (marked with an arrow in Fig. 3b). SYTRON3 shows a moderate accumulation

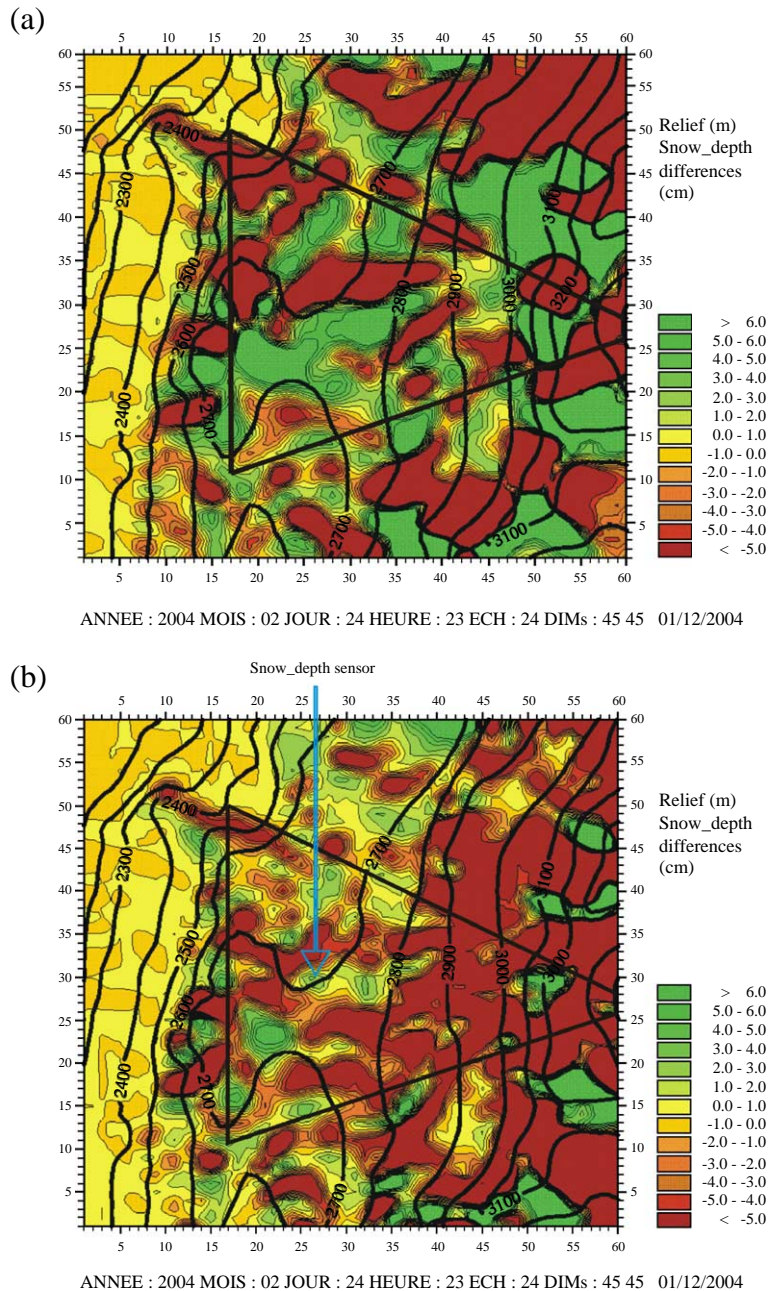


Fig. 3. Comparisons between modeled snow depth differences (cm) for the snow drift event of 24 February 2004. (top (a) : SYTRON2, bottom (b) : SYTRON3). The modeling area is referenced in terms of grid points for each axis. North is towards the top. The distance between grid points is about 45 m. The field of view of the photography (Fig. 2a) is illustrated by a triangle. The terrain is shown by 1 m contour lines. The blue arrow in Fig. 3b indicates the location of the snow depth sensor.



while SYTRON2 suggests for this location no significant change in snow depth; the location is rather situated between two large areas of accumulation and erosion. Fig. 4a shows the observed snow depth and the wind velocity while the corresponding modelled values (SYTRON2 and SYTRON3) are presented in Fig. 3b during the 24h event.

Considering snow depth differences over the whole drift period, the average observed difference is 6.3 cm with maximum changes up to 46 cm. SYTRON3 shows a 3.8 cm difference with a quite continuous growing rate during 16 hours and SYTRON2 with a difference of only 1.2 cm. The horizontal spatial scale of these results must be kept in mind for the interpretation of the comparison between punctually observed snow depths and the modelled snow depth difference fields. The observed

value is only representative of about 1 m<sup>2</sup> while the models are running with grid of about 45 m × 45 m. This quite large mesh size is unable to represent locally large horizontal gradients of snow depth which are usually observed at small scale in the studied area. Thus, the modelling mesh size induces a lower amplitude and has an obvious smoothing effect on plotted modelled fields. In accordance with the observation, the models well simulate the end of the blowing period after 15 hours. However, the shapes of the modelled snow depth curves are still rather different during the event from the observed snow depth. Two consecutive cycles of accumulation and erosion were measured at the location of the snow depth sensor during the snow drift event while the models only show a continuous increase during the same period. The underlying assumptions

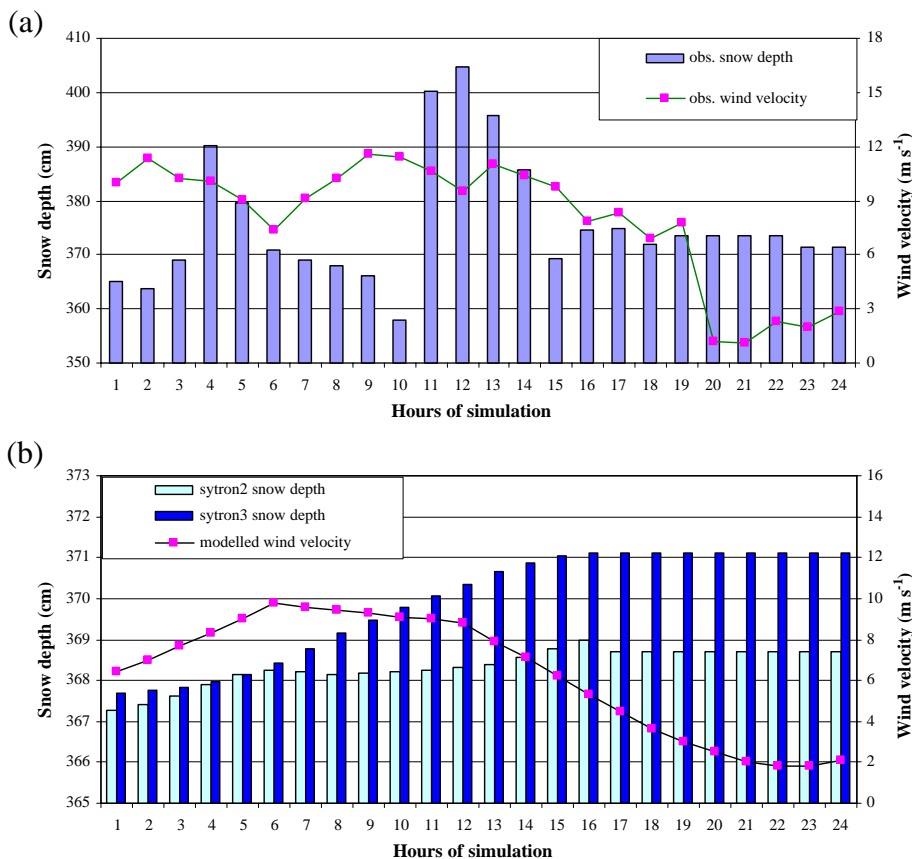


Fig. 4. (a) Snow depth and wind velocity measured at the location indicated by the blue arrow in Fig. 3 for 24 hours beginning at 24 February 2004 at 00 UTC. (b) Model results : snow depth from SYTRON2 and SYTRON3 and wind velocity modeled by SAMVER.

Table 1

Snow depth differences observed at the site of the snow depth sensor and modelled (by SYTRON2 and SYTRON3) during the main snow drift events

Date	Snow depth difference (cm)			Duration of snow drift event (h)
	SYTRON3	SYTRON2	OBSERVED	
21 January 2004	+4	−5	+18	24 h
8 February 2004	−3	−4	−3	24 h
24 February 2004	+4	+1	+6	15 h
12 March 2004	−9	+8	−18	18 h
16 April 2004	−1	+1	−5	6 h

The location of the snow depth sensor is indicated by an arrow in Fig. 3.

in our models do not allow to capture these temporal features. Another limiting reason is the modelled velocity profile for the location of the snow depth sensor as shown in Fig. 4b. Its smoothed appearance is far different from the corresponding observed values as seen in Fig. 4a; this is mainly due to the previously presented insufficiencies of the model SAMVER (only one computation level) and of its temporal coupling with the large scale wind velocity modelled by the SCM forecasting chain every 6 hours. Therefore, the modelled wind velocity cannot reproduce finely the observed profile and deviates on average over the period by  $1.7 \text{ m s}^{-1}$ .

Table 1 summarizes the comparisons, between modelled and observed snow depth differences at the location of the snow depth sensor during all the main identified snow drift events of the 2004 winter season including the previously discussed event. One can see a clear advantage of the SYTRON3 model; even if the amplitude of the event is systematically underestimated by SYTRON3, it always properly identifies accumulation or erosion periods which is not the case for SYTRON2.

## 5. Conclusions

The new version of the snow drift model, called SYTRON3, which is implemented in the operational avalanche forecasting model chain Safran-Crocus-Mepra, is more physically based and shows more fine scale details when compared to the previous version (SYTRON2). A better determination of the average snow deposition during a snow drift period has been achieved. However, the fine scale temporal evolution during the snow drift period could not be

simulated according to the observations. The main improvements are as follows:

- An improved estimation of the wind field while keeping the coupling with the operational SCM model forecasting chain and without using local observations except for validation and control.
- An improved description of the physical processes involved in the snow drift process by introducing more realistic parameterisations.

The main goal remains to develop an operational tool, which requires limited computer time and is able to simulate snow drift at various alpine locations without local observations. The preliminary results presented demonstrate the potential of the tool for operational applications. In the future, the estimation of the albedo from photography should be improved by considering the anisotropy of the reflected radiation and by applying different techniques of image processing in order to identify features related to snow drift events.

## Acknowledgements

We are grateful to the management and personnel of the safety service of the Alpe d'Huez ski resort who helped to maintain the observation site. Special thanks are given to Philippe Puglièse who is in charge of the instrumentation of the site, to Delphine Charlieu and Dominique Lecorps for their help with photographic treatments and techniques. We thank the editor and the referees for their detailed and meticulous revisions of the paper form, content and language, and for their helpful suggestions which

greatly improved the final version. We are also indebted to friends and colleagues for useful comments and suggestions.

## References

- Castelle, T., 1995. Transport de la neige par le vent en montagne: approche expérimental du site du Col du Lac Blanc [Grandes Rousses, France]. Thèse no 1303 sc. techn. EPF Lausanne, 1995. XII, 255 p. III. N2222.
- Corripio, J.G., 2004. Snow surface albedo estimation using terrestrial photography. *International Journal of Remote Sensing* 25 (24), 5705–5729.
- Corripio, J.G., Durand, Y., Guyomarc'h, G., Mérindol, L., Lecorps, D., Puglièse, P., 2004. Land-based remote sensing of snow for the validation of a snow transport model. *Cold Regions Science and Technology* 39 (2004), 93–104.
- Durand, Y., Giraud, G., Brun, E., Mérindol, L., Martin, E., 1999. A computer-based system simulating snowpack structures as a tool for regional avalanche forecast. *J. Glaciol.* 45 (151), 466–484.
- Durand, Y., Guyomarc'h, G., Mérindol, L., 2001. Numerical experiments of wind transport over a mountainous instrumented site. (Part. 1: Regional scale). *Ann. Glaciol.* 32, 187–195.
- Durand, Y., Guyomarc'h, G., Mérindol, L., Corripio, J.G., 2004. 2D numerical modelling of surface wind velocity and associated snowdrift effects over complex mountainous topography. *Ann. Glaciol.* 38, 59–71.
- Gallée, H., Guyomarc'h, G., Brun, E., 2000. Impact of snowdrift on the Antarctic Ice Sheet surface mass balance: possible sensitivity to snow-surface properties. *Boundary-Layer Meteorology* 99, 1–19.
- Gauer, P., 2001. Numerical modelling of blowing and drifting snow in Alpine terrain. *J. Glaciol.* 47 (156), 97–110.
- Greely, R., Iversen, J.D., 1985. *Wind as a Geological Process on Earth, Mars, Venus and Titan*. Cambridge University Press, Cambridge.
- Guyomarc'h, G., Mérindol, L., 1998. Validation of an application for forecasting blowing snow. *Ann. Glaciol.* 26, 138–143.
- Kind, R.J., 1976. A critical examination of the requirements for model simulation of wind-induced erosion/deposition phenomena such as snow drifting. *Atmos. Environ.* 10 (3), 219–227.
- Kind, R.J., 1992. One-dimensional aeolian suspension above beds of loose particles—a new concentration profile equation. *Atmos. Environ.* 26A (5), 927–931.
- Lehning, M., Doorschot, J., Fierz, C., Raderschall, N., 2002. A 3D model for snow drift and snow cover development in steep alpine terrain. In: Stevens, J.R. (Ed.), *Proceedings ISSW 2002. International Snow Science Workshop, Penticton BC, Canada, 29 September–4 October 2002*, pp. 579–586.
- Liston, G.E., Sturm, M., 1998. A snow-transport model for complex terrain. *J. Glaciol.* 44 (148), 498–516.
- Naaim, M., Naaim-Bouvet, F., Martinez, H., 1998. Numerical simulation of drifting snow: erosion and deposition models. *Ann. Glaciol.* 26, 191–196.
- Pomeroy, J.W., Gray, D.M., 1990. Saltation of snow. *Water Resour. Res.* 26 (7), 1583–1594.
- Owen, P.R., 1964. Saltation of uniform grain in air. *J. Fluid Mech.* 20 (2), 225–242.
- Wiscombe, W.J., Warren, S.G., 1980. A model for the spectral albedo of snow: I. Pure snow. *J. Atmos. Sci.* 37, 2712–2733.